Among CXCR3 Chemokines, IFN-γ-Inducible Protein of 10 kDa (CXC Chemokine Ligand (CXCL) 10) but Not Monokine Induced by IFN-γ (CXCL9) Imprints a Pattern for the Subsequent Development of Autoimmune Disease[1]

Urs Christen,[2]* Dorian B. McGavern,[†] Andrew D. Luster,[‡] Matthias G. von Herrath,* and Michael B. A. Oldstone[†]

Infection of the pancreas with lymphocytic choriomeningitis virus results in rapid and differential expression among CXCR3 chemokines. IFN-γ-inducible protein of 10 kDa (IP-10), in contrast with monokine induced by IFN-γ and IFN-inducible T cell-α chemoattractant, is strongly expressed within 24 h postinfection. Blocking of IP-10, but not monokine induced by IFN-γ, aborts severity of Ag-specific injury of pancreatic β cells and abrogates type 1 diabetes. Mechanistically, IP-10 blockade impedes the expansion of peripheral Ag-specific T cells and hinders their migration into the pancreas. IP-10 expression was restricted to viruses infecting the pancreas and that are capable of causing diabetes. Hence, virus-induced organ-specific autoimmune diseases may be dependent on virus tropism and its ability to alter the local milieu by selectively inducing chemokines that prepare the infected tissue for the subsequent destruction by the adaptive immune response. ***The Journal of Immunology,*** **2003, 171: 6838–6845.**

Viruses can induce inflammation and autoimmune disease. Inflammation is initially orchestrated by chemokines and cytokines that form an integral part of the innate immune system. First, they attract and activate an array of leukocytes with the goal of controlling the invading pathogen until the adaptive immune response is in place. Second, chemokines, through interaction with their corresponding receptors that are differentially expressed on Th1/cytotoxic T lymphocyte (Tc)1-[3] and not Th2/Tc2-type lymphocytes (1, 2), modulate the Th1/Tc1 vs Th2/Tc2 balance and thereby direct the inflammatory response toward a more aggressive Th1/Tc1-phenotype that is required for the elimination of intracellular organisms, such as viruses. For example, the chemokine receptors CXCR3 and CCR5 are associated with a Th1/Tc1 phenotype (3–5), whereas CCR3, CCR4, and CCR8 are found on Th2/Tc2-type lymphocytes (4–7).

Based on the dominance of Th1/Tc1 cells in driving various immunopathological diseases, we questioned how Th1/Tc1 chemokines expressed during an initial inflammatory process induced by a virus influenced the development of immune-mediated diseases. As a model system, we used acute lymphocytic choriomeningitis virus (LCMV) infection of transgenic mice that expressed the glycoprotein (GP) of LCMV in the β cells of the islets of Langerhans (rat insulin promotor (RIP)-GP mice) (8, 9). LCMV was chosen because it does not lyse the cells it infects; it generates of an impressive antiviral immune response, and disease associated with LCMV infection is exclusively mediated by the antiviral immune response. RIP-GP transgenic mice were selected as the host because the expression of the target Ag (LCMV-GP transgene) is restricted to the islets of Langerhans in the pancreas, which facilitates measurement and quantification of the biochemical and pathologic phenotype. RIP-GP mice do not develop type 1 diabetes spontaneously; however, upon infection with LCMV, >95% of the RIP-GP mice develop a rapid disease onset as determined by a blood glucose concentration of >300 mg/dl, massive T cell infiltration restricted to the islets, and destruction of β cells with resultant low to absent pancreatic insulin levels (9, 10). Concurrent with LCMV-mediated immunopathological diabetes is a profound Th1/Tc1-type response characterized by the release of the proinflammatory cytokines IFN-γ and TNF-α in the target organ (11, 12) and a β cell destructive process that is dependent on CD8 T cells specific for LCMV-GP (9, 10).

After i.v. or i.p. LCMV infection, a modest replication of virus is found in the pancreas (13). We now document that within the first 18–24 h after virus inoculation, CXCR3 chemokines are differentially expressed. IFN-γ-inducible protein of 10 kDa (IP-10; CXC chemokine ligand (CXCL) 10), in contrast with the other CXCR3 chemokines, monokine induced by IFN-γ (Mig; CXCL9) and IFN-inducible T cell-α chemoattractant (I-TAC; CXCL11), is highly expressed and plays a dominant role in programming the ensuing autoimmune disease. The onset and kinetics of IP-10 expression observed in the pancreas are unique and markedly contrast in three respects with previous reports of IP-10 expression

*Department of Developmental Immunology, La Jolla Institute for Allergy and Immunology, San Diego, CA 92121; †Department of Neuropharmacology, The Scripps Research Institute, La Jolla, CA 92037; and ‡Center for Immunology and Inflammatory Diseases, Division of Rheumatology, Allergy and Immunology, Massachusetts General Hospital, Harvard Medical School, Charlestown, MA 02129

Received for publication June 20, 2003. Accepted for publication October 7, 2003.

The costs of publication of this article were defrayed in part by the payment of page charges. This article must therefore be hereby marked *advertisement* in accordance with 18 U.S.C. Section 1734 solely to indicate this fact.

[1] This work was supported by a fellowship from the Juvenile Diabetes Foundation (3-2000-510 to U.C.), by National Institutes of Health Training Grant AG00080 (to D.B.M.), by National Institutes of Health Grant AI41439 (to M.B.A.O.), by National Institutes of Health Grant R01A69212 (to A.D.L.), and by National Institutes of Health Grant R29DK51091 (to M.G.V.H.). This is Publication Number 15151-NP from the Division of Virology, Department of Neuropharmacology, The Scripps Research Institute.

[2] Address correspondence and reprint requests to Dr. Urs Christen, Department of Developmental Immunology, DI-3, La Jolla Institute for Allergy and Immunology, 10355 Science Center Drive, San Diego, CA 92121. E-mail address: christen@liai.org

[3] Abbreviations used in this paper: Tc, cytotoxic T lymphocyte; LCMV, lymphocytic choriomeningitis virus; GP, glycoprotein; RIP, rat insulin promotor; IP-10, IFN-γ-inducible protein of 10 kDa; Mig, monokine induced by IFN-γ; I-TAC, IFN-inducible T cell-α chemoattractant; GFP, green fluorescent protein; CVB, Coxsackievirus B4; EMC-B, encephalomyocarditis virus variant B; TV, Theiler's murine encephalomyelitis virus; RPA, RNase protection assay; MIP, macrophage-inflammatory protein.

0022-1767/03/$02.00

after infection with a variety of viruses of the CNS (14–16). First, in CNS infection a battery of chemokines is elevated without a clear preference to any one. Second, chemokine expression occurs later at days 5–7. Third, there is no dominance for IP-10 expression. Our data demonstrate that IP-10 was selectively enhanced in infected RIP-LCMV mice and that neutralization of IP-10, but not Mig, blocked the virus-induced immune-mediated disease.

Using a novel assay with LCMV-GP-specific CD8 T cells expressing green fluorescent protein (GFP), we could determine the mechanism(s) by which blockade of IP-10 significantly lowered the incidence of autoimmune type 1 diabetes. First, a decrease in the clonal expansion of Ag-specific CD8 T cells was observed and, second, the recruitment of such autoaggressive T cells into the islets of Langerhans was found to be significantly lowered. Hence, IP-10 is a critical determinant for the migration of Ag-specific CD8 T cells into the target organ and is required to initiate the subsequent development of immune-mediated disease. In addition, IP-10 expression in the pancreas is a general phenomenon, in that infection of mice with viruses that are tropic for the pancreas and are known to cause diabetes, such as Coxsackievirus B4 (CVB) and encephalomyocarditis virus variant B (EMC-B), resulted in high-level pancreatic expression of IP-10 at days 1–4 postinfection. In contrast, infection with Theiler's murine encephalomyelitis virus (TV), a virus without pancreas tropism that does not cause diabetes, did not result in the expression of significant levels of IP-10 in pancreas.

Materials and Methods

Mice, viruses, and Abs

Generation of H-2^b RIP-LCMV-GP transgenic mice has been described previously (9, 10). The presence of transgenic RIP-GP sequences was determined by performing standard PCR with genomic DNA obtained from mouse tails as described (12). Generation of GFP × TCR($GP_{33–41}$) double transgenic mice has been described (17). Briefly, C57BL/6-TgN(ACTbEGFP)1Osb mice (GFP mice; The Jackson Laboratory, Bar Harbor, ME) that express GFP under the control of the β-actin promoter (18) were crossed with B6;D2-TgN(TcRLCMV)327Sdz mice that express a $D^b(GP_{33–41})$-specific TCR (19). The Armstrong clone 53b strain of LCMV was used for all experiments. LCMV was plaque purified three times on Vero cells, and stocks were prepared by a single passage on hamster kidney fibroblast cell line BHK-21 (ATCC CCL-10, American Type Culture Collection, Manassas, VA) cells. Mice were infected with a single i.p. dose of 5×10^3 PFU. CVB and EMC-B (20) were kindly provided by Dr. J. L. Whitton (The Scripps Research Institute, La Jolla, CA) and Dr. A. L. Notkins (National Institutes of Health, Bethesda, MD), respectively. The hamster anti-murine IP-10 mAb (1F11) was generated and purified as described (21) and was administered at 100 μg in 100 μl of PBS per injection 6 h before and then at days 1, 2, 4, and 6 after LCMV infection. The hamster anti-murine Mig hybridoma (2A6.9.9) was a kind gift from Dr. R. Schreiber (Washington University School of Medicine, St. Louis, MO). This anti-Mig mAb specifically neutralized murine Mig function (A. D. Luster, unpublished observations) and was produced and purified in parallel using the same conditions as the anti-IP-10 mAb (21). As a control, a group of four mice were injected with an isotype-matched hamster IgG Ab (Southern Biotechnology Associates, Birmingham, AL). For blocking of RANTES, a neutralizing monoclonal anti-RANTES Ab from R&D Systems (Minneapolis, MN) was used. The polyclonal rabbit anti-CXCR3 Ab was purchased from Zymed Laboratories (South San Francisco, CA) and the anti-IFN-γ mAb was obtained from BD PharMingen (San Diego, CA).

Blood glucose (BG) measurements

Blood samples were obtained from the retro-orbital plexus and plasma glucose concentration was determined using a ONE TOUCH Ultra glucometer (LifeScan, Milpitas, CA). Mice with BG values of 300 mg/dl or higher were considered diabetic (22).

RNase protection assay (RPA)

Total RNA was isolated from whole pancreas homogenates using Tri-Reagent (Molecular Research Center, Cincinnati, OH). RNA was extracted with chloroform followed by isopropanol precipitation and washing with ethanol. Twenty micrograms of total pancreatic RNA was used for hybridization with a ^{32}P-UTP-labeled multitemplate set containing specific probes for various chemokines (Riboquant, mCK-5; BD PharMingen). Specific probes for IP-10, Mig, I-TAC, and CXCR3 were kindly provided by Iain Campbell and Valerie Asensio (The Scripps Research Institute). The RPA was conducted according to the manufacturer's guidelines. The resulting analytical acrylamide gel was scanned using a STORM-860 PhosphorImager (Molecular Dynamics, Sunnyvale, CA), and the intensity of bands corresponding to protected mRNA was quantified using ImageQuant image analysis software (Molecular Dynamics) and L32 as a reference gene.

Immunohistochemistry

Organs were harvested, immersed in Tissue-Tek OCT (Bayer, Elkhart, IN), and quick frozen on dry ice. Six- to ten-micrometer tissue sections were cut using a cryomicrotome and placed onto sialin-coated Superfrost Plus slides (Fisher Scientific, Pittsburgh, PA). Sections were fixed with 90% EtOH at −20°C, and after washing in PBS an avidin-biotin blocking step was performed (Vector Laboratories, Burlingame, CA). Primary and biotinylated secondary Abs (Vector Laboratories) were incubated on the sections for 30 min each, and the color reaction was obtained by sequential incubation with an avidin-peroxidase conjugate (Vector Laboratories) and diaminobenzidine-hydrogen peroxide. Primary Abs were rat anti-mouse CD8a (Ly2), rat anti-mouse CD8b (Ly3), rat anti-mouse CD4 (BD PharMingen), and rat anti-mouse F4/80 (Serotec, Raleigh, NC).

Adoptive transfer of GFP-($GP_{33–41}$) T cells

GFP-$D^b(GP_{33–41})$ T cells were purified from the spleens of GFP × TCR($GP_{33–41}$) double transgenic mice by negative selection (StemCell Technologies, Vancouver, BC, Canada). After the enrichment procedure, it was determined that 98% of the GFP-positive cells were $CD8^+$. A total of 10^4 GFP-$D^b(GP_{33–41})$ T cells in 100 μl of PBS were injected i.v. into naive RIP-GP mice. Two days later, the mice were infected with 5×10^3 PFU of LCMV. Anti-IP-10 mAb was administered 6 h before infection and then at days 1, 2, 4, and 6 postinfection. At day 8 postinfection, mice were sacrificed, and blood and spleen were removed for analysis of GFP-$D^b(GP_{33–41})$-specific T cells by flow cytometry. After removal of the blood and spleen, mice received an intracardiac perfusion with 30 ml of 4% paraformaldehyde (in PBS). Pancreata were removed, weighed, incubated in 4% paraformaldehyde (4°C, 24 h), and then incubated for an additional 24 h (4°C) in 30% sucrose. After freezing tissues in OCT, a single 6-μm frozen section was cut from each pancreas, stained with 4′,6′-diamidino-2-phenylindole (1 μg/ml, 5 min, room temperature; Sigma-Aldrich, St. Louis, MO) to visualize nuclei, and analyzed by fluorescence microscopy to obtain the total number of infiltrating GFP-$D^b(GP_{33–41})$ T cells. Reconstructions of pancreas sections were accomplished using an Axiovert S100 immunofluorescence microscope (Zeiss, Oberkochen, Germany) fitted with an automated *xy* stage, an Axiocam color digital camera, and a 5× objective. Registered two-color images (4′,6′-diamidino-2-phenylindole and GFP) were captured for each field on pancreas sections, and reconstructions were performed using the MosaiX function in the K300 image analysis software (Zeiss). The total number of GFP-$D^b(GP_{33–41})$ T cells per pancreas was calculated based on the organ weight. In the KS300 image analysis program, reconstructions of pancreas sections were used to calculate the percentage of tissue occupied by GFP signal. This percentage was multiplied by the organ volume and then divided by the average volume of a single T cell to obtain the total number of GFP-$D^b(GP_{33–41})$ T cells per pancreas. As a background control, the same procedure was performed on a mouse that did not receive an adoptive transfer of GFP-$D^b(GP_{33–41})$ T cells. Analysis of the GFP signal in the control pancreas resulted in the detection of no cells. Statistical analyses of flow cytometry and pancreas data were performed using a Student's *t* test.

Results

Pancreatic chemokine expression after infection with LCMV

To examine the kinetics and pattern of pancreatic chemokine expression, we isolated total RNA from pancreata of either RIP-GP or wild-type C57BL/6 mice at different times after i.p. infection with 5×10^3 PFU of LCMV-Armstrong. Analysis of 10 different chemokine mRNA species, including the three known CXCR3 chemokines, by RPA revealed a prominent and extensive expression of IP-10 after infection. IP-10 mRNA was detected as early as day 1 after infection, and quantification of the data revealed an elevation by >400-fold (Fig. 1). At day 2, IP-10 expression decreased to less than half of that amount and thereafter dropped rapidly to levels found in an uninfected animal (Fig. 1). In support

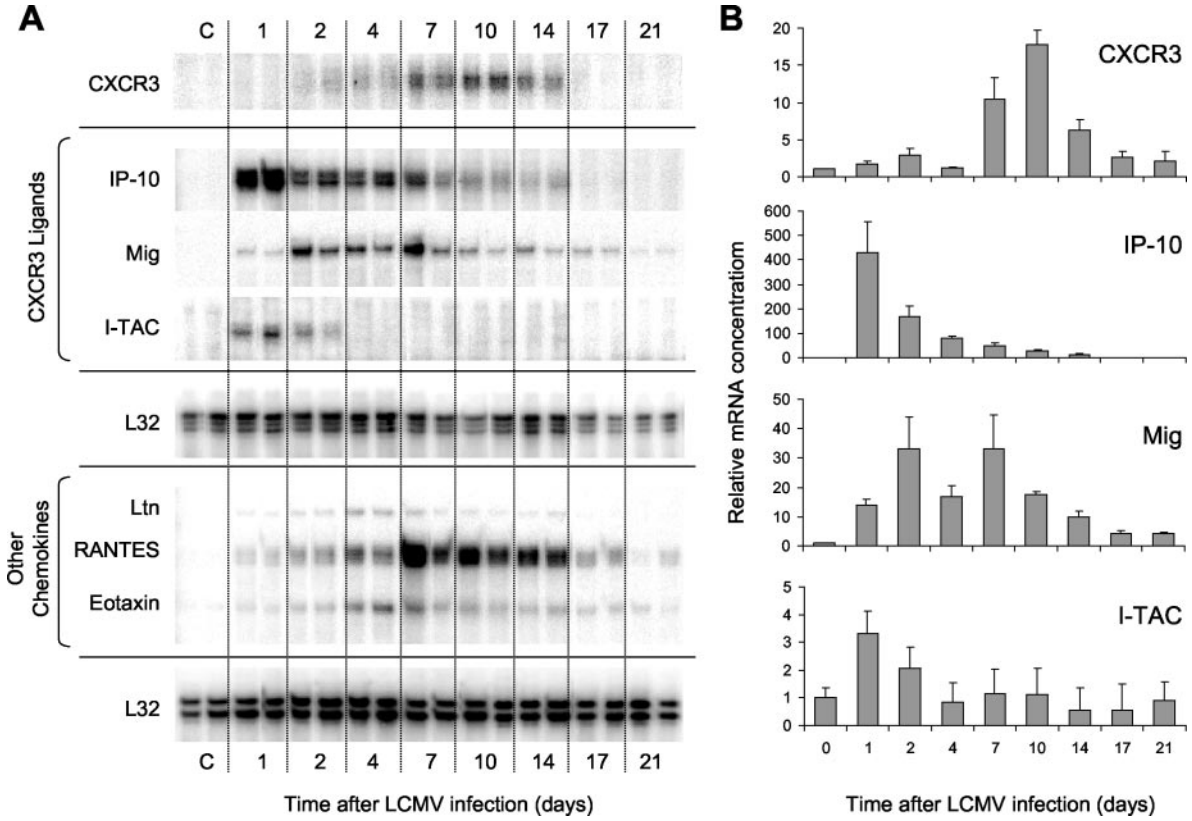

FIGURE 1. Expression of CXCR3 chemokines after LCMV infection. RPA using total RNA isolated from total pancreas homogenates of RIP-GP mice at several times after LCMV infection. Note that the expression profiles of the individual chemokines follow distinct kinetics. *A*, Results obtained from two representative mice per time were assembled for display (total number of mice was four to seven per time). *B*, For quantification of the relative amounts of individual mRNA species, the signal intensities were normalized against L32 and are depicted relative to the mRNA amounts expressed in uninfected mice. Data are mean relative signal intensities (±SEM; $n = 4–7$).

of these data, expression of CXCR3 was detected as early as day 7 after LCMV infection (Fig. 1). Because CXCR3 is expressed predominantly on activated T cells, it is most likely that CXCR3 expression in the pancreas is due to the infiltration of activated T cells that occurs around days 7–10 after LCMV infection (13). Indeed, LCMV-specific CD8 T cells express high levels of CXCR3 at their cell surface. As determined by flow cytometry using a polyclonal anti-CXCR3 Ab, CXCR3 was expressed in ~60% of splenic CD8 T cells of uninfected RIP-GP mice and in ~80% of all CD8 T cells at day 7 after infection of RIP-GP mice with LCMV (Fig. 2*A*). Among activated LCMV-specific CD8 T cells, the percentage of $CXCR3^{high}$ cells was further elevated to 93% (Fig. 2*A*). There was no significant difference in the percentage of $CXCR3^{high}$ CD8 T cells between transgenic RIP-GP and wild-type C57BL/6 mice (Fig. 2*A*).

In contrast with IP-10, expression of Mig had delayed kinetics. Compared with the expression in uninfected mice, Mig mRNA was enhanced ~30-fold between days 2 and 7 after LCMV infection and decreased to baseline levels by day 21 (Fig. 1). I-TAC was expressed with a kinetics similar to that of IP-10 but was only up-regulated threefold over levels expressed in uninfected controls (Fig. 1). The levels and kinetics of IP-10, Mig, and I-TAC expression induced by an acute LCMV infection were equivalent in both C57BL/6 wild-type and RIP-GP transgenic mice. Thus, the chemokine expression observed was a direct result of the viral infection and not the presence of the transgene in the β cells or the adaptive immune response to the virus that is first detected at 5 days after viral inoculation (9, 10). Other chemokines, such as RANTES (CCL5), showed a kinetic profile different from those of the CXCR3 chemokines. Expression of RANTES peaked between days 7 and 10 postinfection, a time corresponding to maximal CD8 T cell infiltration into the pancreas (Fig. 1*A*). Only modest increases of CCL2 (monocyte chemoattractant protein-1), CCL11 (Eotaxin), and CXCL1 (Lymphotactin) were noted (Fig. 1*A*), with no detectable expression of CCL1 (TCA-3), CCL4 (macrophage-inflammatory protein-1β (MIP-1β)), and CXCL2 (MIP-2).

Neutralization of IP-10, but not of Mig, abrogates the development of type 1 diabetes

Because both IP-10 and Mig showed an elevated expression early after LCMV infection (Fig. 1), we next addressed the role of these CXCR3 chemokines in the subsequent development of autoimmune diabetes. To this end, we injected mAbs to either IP-10 or Mig into RIP-GP mice that were infected with 5×10^3 PFU of LCMV. These Abs neutralize IP-10 or Mig, respectively, and were used at concentrations exceeding their neutralizing capacity (see *Materials and Methods*) (21). Ab to either IP-10 or Mig (100 μg of each) was administered i.p. 6 h before LCMV infection and then at days 1, 2, 4, and 6 postinfection. The incidence of diabetes (BG >300 mg/dl) was significantly reduced to 31% in RIP-GP mice that received anti-IP-10 mAb compared with control animals, which were injected with an unspecific isotype-matched hamster Ab or with PBS (incidence of 100%) (Fig. 2*B*). In contrast with IP-10 neutralization, no significant reduction in diabetes incidence or onset could be detected for animals that were treated with the anti-Mig mAb (Fig. 2*B*). In addition, when anti-IP-10 mAb and anti-Mig mAb were coinjected, the incidence of diabetes was equivalent to that observed after administration of anti-IP-10 mAb

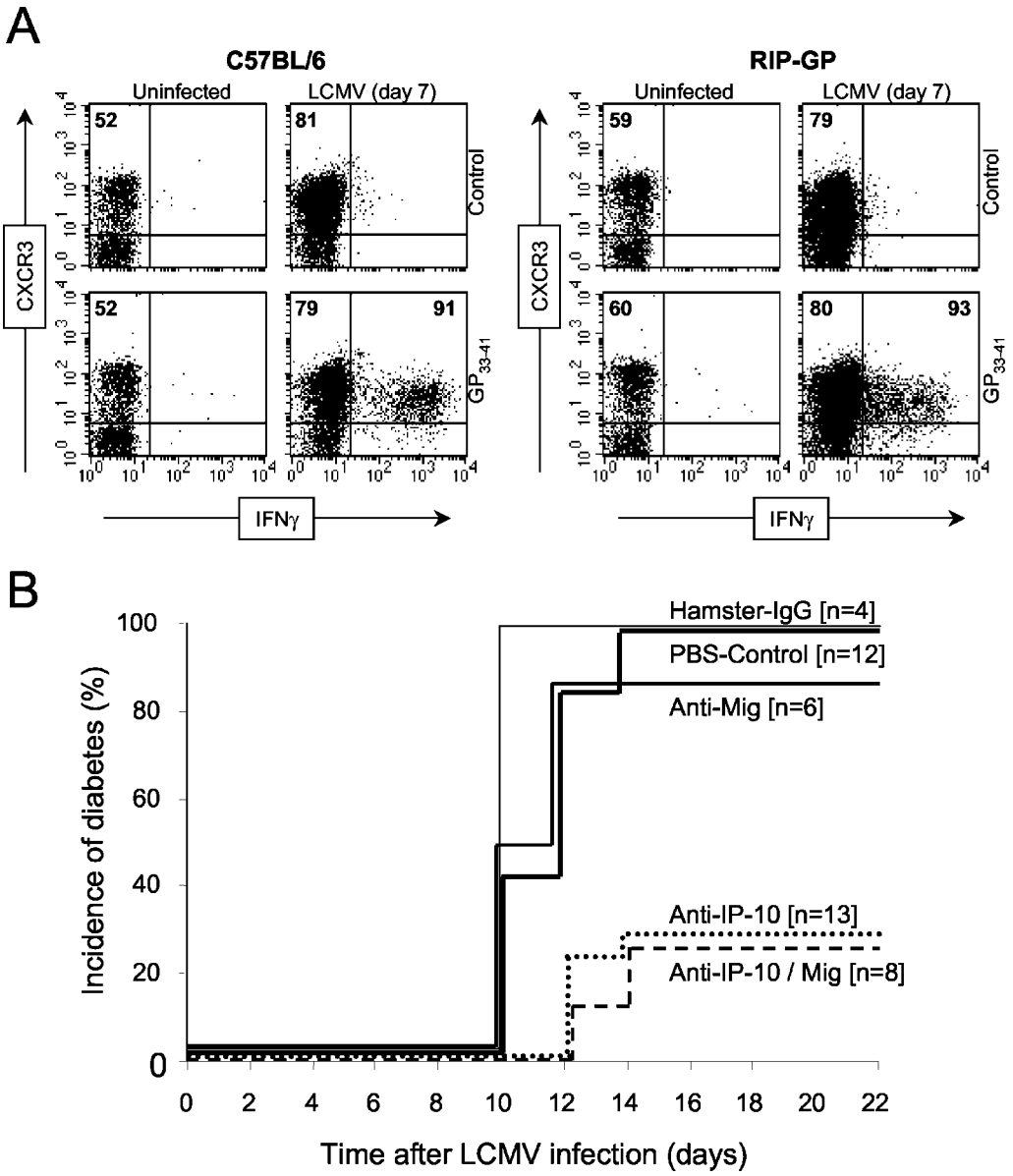

FIGURE 2. Neutralization of IP-10, but not Mig, prevents type 1 diabetes in RIP-GP mice. *A*, CXCR3 expression on LCMV-specific CD8 T cells: splenocytes were isolated from uninfected and LCMV-infected (day 7) RIP-GP or C57BL/6 mice and were stimulated for 5 h with the immunodominant LCMV epitope $GP_{33–41}$ (1 μg/ml) in presence of brefeldin A (2 μg/ml). $GP_{33–41}$ specific CD8 T cells were identified by intracellular IFN-γ staining and were probed for CXCR3 expression with a polyclonal anti-CXCR3 Ab by flow cytometry. Splenocytes were gated for CD8 expression, and the indicated number represents the mean percentage of $CXCR3^{high}$ cells of either IFN-γ^{low} (unspecific) CD8 T cells or IFN-γ^{high} (LCMV-GP-specific) CD8 T cells as detected in three mice per group. *B*, Cumulative incidence of diabetes in five groups of RIP-GP mice infected with LCMV and treated with 100 μg of anti-IP-10 mAb (Anti-IP-10), anti-Mig mAb (Anti-Mig), isotype-matched hamster Ab (Hamster-IgG), or PBS or with both 100 μg of anti-IP-10 mAb and 100 μg of anti-Mig mAb (Anti-IP-10/Mig) at days 0, 1, 2, 4, and 6 postinfection. BG was determined at the days indicated and mice with BG of 300 mg/dl or higher were scored "diabetic."

alone (Fig. 2*B*). The data from these studies indicate that IP-10, but not Mig, is an essential component in the initiation of the process that results in immune-mediated disease. Blockade of RANTES at the time of its highest expression by administration of 100 μg of a neutralizing anti-RANTES Ab at days 4, 7, and 10 postinfection had no effect on the incidence of diabetes (data not shown).

Neutralization of IP-10 results in decreased cellular infiltration into islets and preserved insulin production

To determine the mechanism(s) by which IP-10 neutralization protects against T cell-mediated immunopathology, we first analyzed the degree of cellular infiltration into the islets of Langerhans. Upon receiving Ab to IP-10, RIP-GP mice were sacrificed at 5, 10, and 23 days postinfection. Pancreata were collected and stained by immunohistochemistry for insulin content using an Ab to insulin B chain. At day 5 after LCMV infection, islets from both treated and untreated mice appeared normal, showing no lymphocyte infiltration and robust insulin staining (Fig. 3). By day 10 postinfection, significant differences between these two groups became apparent, as the islets from mice receiving Ab to IP-10 were still morphologically normal, displayed minimal lymphoid cell infiltrates, and retained the ability to produce insulin (Fig. 3). In contrast, age- and sex-matched littermates that did not receive anti-IP-10 therapy showed substantial lymphocyte infiltration and impaired β cell function, as evidenced by both a marked reduction in islet insulin staining and blood glucose concentrations $>$300 mg/dl (Fig. 3*A*).

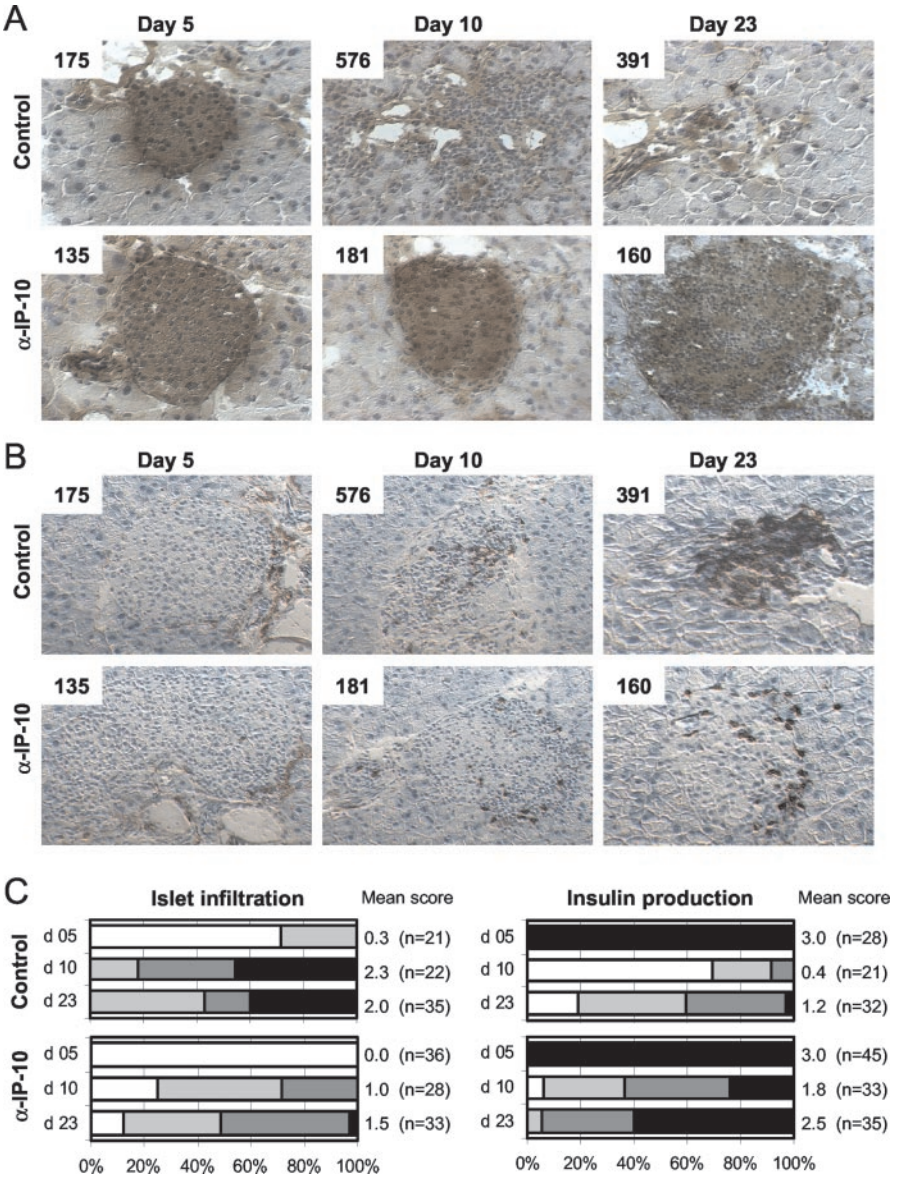

FIGURE 3. Islet infiltration by autoaggressive T cells is inhibited and insulin production is maintained in RIP-GP mice with neutralized IP-10 bioactivity. Pancreas sections of anti-IP-10 mAb treated and untreated RIP-GP mice were obtained at the indicated times after LCMV infection. The sections were stained for insulin production using an anti-insulin B chain Ab (*A*) and using an anti-CD8 Ab for cellular infiltration of CD8 T cells (*B*) and then were counterstained with hematoxylin (representative of $n = 4$). *C*, Islet infiltration and insulin production were scored according to the following system. Islet infiltration (*left panel*): 0, no infiltration, 1, peri-insular infiltration (no intraislet infiltration); 2, minor intraislet infiltration; 3, major intraislet infiltration ("islet scar"). Insulin production (*right panel*): 0, no insulin; 1, $<$50% of cells produce insulin; 2, $>$50% of cells produce insulin; 3, islet is fully functional. The mean score and the number of islets analyzed in tissue sections of four animals per group are indicated.

The cells infiltrating the islets were predominantly of the CD8 (Fig. 3*B*) and CD4 (data not shown) phenotypes, whereas macrophages showed primarily a peri-insular localization (data not shown). By day 23 postinfection, the islets of mice not receiving Ab to IP-10 were destroyed, leaving islet scars consisting mainly of clumped infiltrating cells (CD8/CD4 T cells and macrophages). Negligible to minimal β cells were found that contained insulin (Fig. 3, *A* and *B*). At this same time point, mice treated with Ab to IP-10 showed a marked decrease in CD8/CD4 T cell and macrophage infiltrates as well as morphologically viable islets with insulin expression in the β cells. These findings, concurrent with normal BG levels, indicated that the islets remained functional in the regulation of BG (Fig. 3, *A* and *B*).

Blockade of IP-10 inhibits the expansion and migration of LCMV-specific CD8 T cells into the islets

Previous studies using RIP-GP transgenic mice either genetically or Ab depleted of CD4 and CD8 T cells showed that virus-induced diabetes depends primarily on the expansion and migration of LCMV-specific CD8 T cells into the islets of Langerhans followed by their interactions with β cells expressing the LCMV-GP transgene (10, 23). In C57BL/6 mice (H-2^b background), one of the immunodominant CD8 T cell epitopes residing in the LCMV-GP was identified as amino acids 33–41 (24–26). Furthermore, the GP_{33-41} peptide can be administrated to tolerize and prevent immune-mediated diabetes after LCMV infection (27, 28).

Because CD8 T cells specific for GP_{33-41} are required to cause diabetes in H-2^b RIP-GP transgenic mice, we next asked whether IP-10 neutralization interfered with the expansion of Ag-specific CD8 T cells and/or their migration into the pancreas. Two complementary approaches were used to visualize and enumerate H-$2D^b$ restricted GP_{33-41}-specific CD8 T cells in target tissues infected by LCMV (17). First, using in situ MHC class I tetramer staining (17, 29, 30), it was determined that the frequency of GP_{33-41}-specific CD8 T cells in the islets of RIP-GP mice during the effector phase of the disease (days 7 and 10) was surprisingly only 1% of the total infiltrating CD8 T cell population (D. B. McGavern, U. Christen, M. G. von Herrath, and M. B. A. Oldstone, manuscript in preparation). The second approach involved adoptive transfer of $D^b(GP_{33-41})$-specific TCR transgenic cells genetically tagged with GFP (17). This technique has an advantage over the in situ tetramer staining, because it allows one to increase the frequency of Ag-specific T cells in the islets to $>$1%, thus facilitating quantification and comparisons between experimental and control

groups. In addition, the number of specific CD8 T cells that have migrated into the pancreas can be easily visualized and quantified because of the GFP tag (see *Materials and Methods* for details) (17). A total of 10^4 GFP-$D^b(GP_{33-41})$-specific T cells were adoptively transferred i.v. into naive RIP-GP mice, which were infected 2 days later with 5×10^3 PFU of LCMV. Ab to IP-10 was administered as described above. At day 8 after infection, we first harvested blood and spleen for the assessment of GFP-$D^b(GP_{33-41})$-specific T cell frequencies and second performed a cardiac perfusion to analyze the number of infiltrating GFP-$D^b(GP_{33-41})$-specific T cells in the pancreas of the same individual animal. We found that neutralization of IP-10 significantly reduced the numbers of GFP-$D^b(GP_{33-41})$-specific T cells in the spleen and blood at day 8 after infection. In untreated RIP-GP mice, GFP-$D^b(GP_{33-41})$-specific T cells expanded to account for 51% and 49% of all CD8 T cells in the blood and spleen, respectively. In contrast, there was a reduction of GFP-$D^b(GP_{33-41})$-specific CD8 T cells by 31% in the blood and 33% in the spleen of mice treated with Ab to IP-10 (Fig. 4*A*) ($p < 0.05$). Next, the total number of GFP-$D^b(GP_{33-41})$-specific CD8 T cells in the pancreas were enumerated using fluorescence microscopy and an image analysis program (see *Materials and Methods* for details). At day 8 postinfection, GFP-$D^b(GP_{33-41})$-specific CD8 T cells were found in the islets as well as the exocrine pancreas of both Ab to IP-10 treated and untreated mice (Fig. 4, *C* and *D*). However, the RIP-GP mice that received Ab to IP-10 displayed a statistically significant reduction ($p < 0.05$) in the total number of GP_{33-41}-specific CD8 T cells in the pancreas. Untreated RIP-GP mice had an average of 2.1×10^6 GP_{33-41}-specific CD8 T cells in their pancreas, whereas only 1.2×10^6 GP_{33-41}-specific CD8 T cells were found in the pancreata of mice treated with Ab to IP-10 (Fig. 4*B*). Interestingly, the reduction in migration of Ag-specific CD8 T cells into the pancreas (45% reduction) exceeded the reduction observed in the blood (31% reduction) and the spleen (33% reduction) (Fig. 4*B*).

Pancreatic expression of IP-10 is a general phenomenon after viral infection of the pancreas

The last series of experiments compared the ability of viruses that were tropic for the pancreas and cause diabetes with a virus that is not tropic for the pancreas and does not induce diabetes for early pancreatic expression of IP-10. At day 1 after infection, high levels of IP-10 could be detected in mice infected with the pancreas tropic viruses: LCMV strains Armstrong and Pasteur as well as EMC-B (Fig. 5). In addition, infection with a sublethal dose of the pancreas tropic CVB showed a massive expression of IP-10 at day 4 postinfection (Fig. 5). In contrast, infection with TV, which is not tropic for the pancreas, did not result in the expression of significant pancreatic IP-10 levels at days 1 or 4 after infection (Fig. 5). These data indicate that enhanced IP-10 expression in the pancreas is a general phenomenon for viruses associated with causing diabetes. Furthermore, the data suggest that virus tropism for the pancreas and alteration of that target tissue's local milieu by induction of selected chemokines, such as IP-10, may be an initial step that imprints a pattern for the subsequent development of tissue/organ-specific autoimmune diseases caused by viruses.

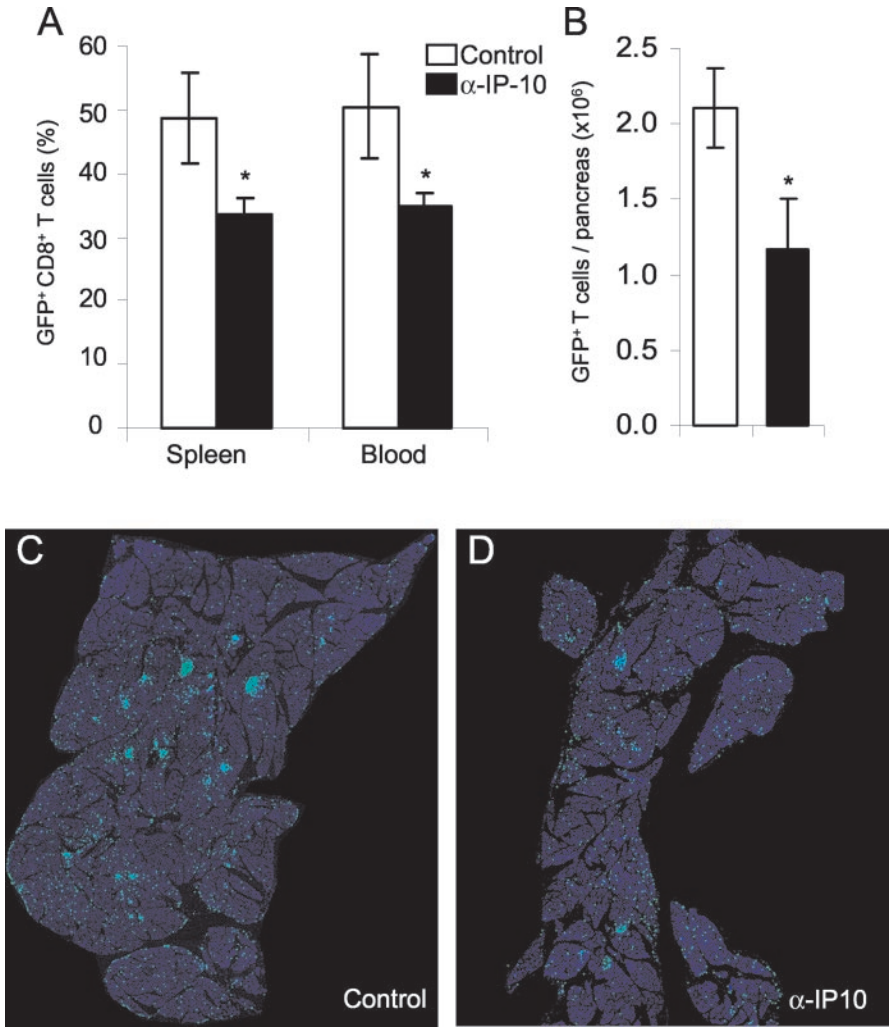

FIGURE 4. Trafficking of LCMV-specific CD8 T cells into the islets of Langerhans is reduced in IP-10-blocked RIP-GP mice. *A*, Frequencies of GFP-$D^b(GP_{33-41})$ CD8 T cells were calculated in the blood and spleen of control ($n = 4$) and anti-IP-10 mAb ($n = 4$)-treated RIP-GP mice at day 8 postinfection. Asterisks denote statistical significance using a Student's *t* test ($p < 0.05$). *B*, The total number of GFP-$D^b(GP_{33-41})$ CD8 T cells in the pancreas was calculated for the same mice shown in *A*. Asterisks denote statistical significance using a Student's *t* test ($p < 0.05$). *C* and *D*, Representative examples of pancreas reconstructions are shown for a control (*C*) and an anti-IP-10 mAb (*D*) treated mouse. Nuclei are shown in blue, and GFP-$D^b(GP_{33-41})$ CD8 T cells are shown in green. Ag-specific CD8 T cell infiltration was significantly reduced but not completely inhibited in anti-IP-10 mAb mice.

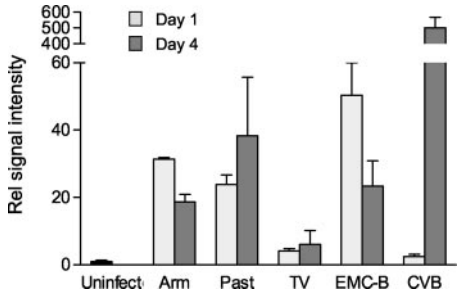

FIGURE 5. Early expression of IP-10 in the pancreas occurs after infection of mice with various viruses tropic for the pancreas. RPA using total RNA isolated from total pancreas homogenates of RIP-GP mice at days 1 and 4 after infection with the following viruses: 1) pancreas tropic, 10^5 PFU (i.p.) of LCMV strain Armstrong (Arm), 10^5 PFU (i.p.) of LCMV strain Pasteur (Past), 10^5 PFU of EMC-B, 10^3 PFU of CVB; 2) non-pancreas tropic, 10^6 PFU (i.p.) of TV. For quantification of the relative amounts of individual mRNA species, the signal intensities were normalized against L32 and are depicted relative to the mRNA amounts expressed in uninfected mice. Data are mean relative signal intensities ($\pm$SEM; $n = 2$–4).

Discussion

In the present study, we report three new findings. First, infection with LCMV caused an immediate expression of CXCR3 chemokines in the pancreas of RIP-GP and wild-type C57BL/6 mice. However, the kinetics and intensity of expression differed among the CXCR3 chemokines. A substantial and early expression of IP-10 was observed that exceeded the expression of Mig by 40-fold and that of I-TAC by 100-fold. Second, neutralization of one CXCR3 chemokine, IP-10, but not Mig, with a blocking mAb abrogated the immune-mediated type 1 diabetes normally observed in LCMV-infected RIP-GP mice. Third, IP-10 blockade interfered with the development of autoimmune diabetes by decreasing the clonal expansion of LCMV-specific CD8 T cells and their migration into the pancreas. The results we report in this study are general, in that an early and elevated expression of IP-10 was observed after infection with several RNA viruses that are tropic for the pancreas and capable of causing diabetes. In contrast, a nondiabetic virus fails to induce significant IP-10 levels in the pancreas. Our composite data indicate that viral infection initially imprints a pattern in the target organ by altering its milieu with triggering specific components of the innate immune response. This early innate immune response in the target organ is apparently an essential component that provides the milieu for the adaptive immune response that is ultimately responsible for causing the pathologic injury.

Previous studies reported CXCR3 chemokine expression after infection of the CNS with viruses such as LCMV (15), mouse hepatitis virus (14, 31), and TV (16). In contrast with the findings we report here, that CXCR3 chemokines are maximally expressed during the first few days after infection of the pancreas with LCMV and precede expression of other chemokines, these same chemokines were expressed later (days 3–11) in the CNS and were made in concert with several other chemokines (e.g., monocyte chemoattractant protein-1, RANTES, MIP-1α, and MIP-1β) (14–16). Because of the unique and elevated pancreatic expression of CXCR3 chemokines (IP-10 and Mig) early after LCMV infection and the high expression of CXCR3 on the surface of LCMV-specific CD8 T cells, we hypothesized that neutralization of IP-10 and/or Mig would limit the development of an LCMV-specific CD8 T cell response that ultimately causes autoimmune diabetes. Indeed, injection of a neutralizing anti-IP-10 mAb during the time of maximal IP-10 expression significantly reduced the anti-LCMV specific CD8 T cell response as well as the incidence of type 1 diabetes in RIP-GP mice. In addition, a unique and nonredundant role for IP-10 was revealed, because it was not possible to abrogate diabetes by treatment with a neutralizing anti-Mig mAb. Moreover, coadministration of anti-Mig and anti-IP-10 mAbs did not decrease further the incidence of diabetes observed with anti-IP-10 mAb treatment alone. These data indicate distinct roles for IP-10 and Mig in the initiation of a virus-induced immune-mediated diabetes.

Although both IP-10 and Mig were expressed at an early stage after LCMV infection, expression of Mig followed a different kinetic pattern than did IP-10 expression. Peak expression of Mig occurred later, at a time concurrent with the expression of other chemokines (RANTES; see Fig. 1) and proinflammatory cytokines (TNF-α and IFN-γ) (11, 12). Hence, it appears that the timing of immunotherapy will be critical for the successful prevention of immune-mediated disease, and possibly in contrast with early IP-10 neutralization, blockade of Mig might inhibit just one of many factors that influence the local inflammatory profile at a later time point. Importantly, despite the multiplicity of chemokine and cytokine release during inflammation and the likely redundancy in the system, we show here that neutralization of just one chemokine, IP-10, is able to abort an immune-mediated disease.

The dominant role of CXCR3 chemokines after microbial infection is not unexpected, because CXCR3 is expressed predominantly on activated T cells (32, 33), which function to eliminate virus-infected cells and to control viral infection. Furthermore, there is considerable evidence that CXCR3 chemokines are important mediators of Th1/Tc1-type inflammation processes. For example, neutralization of IP-10 inhibited the massive migration of T cells into the liver and spleen that normally follows infection of mice with *Toxoplasma gondii* (21). Impaired Ag-specific T cell effector function was also observed, indicating that IP-10 plays a central role in localization and function of effector T cells at sites of Th1/Tc1 inflammation (21). Similar results have been obtained using IP-10-deficient (IP-$10^{-/-}$) mice (34). After infection with a neurotropic mouse hepatitis virus, IP-$10^{-/-}$ mice had a decreased recruitment of CD4 and CD8 T cells to the brain and reduced numbers of virus-specific IFN-γ-secreting CD8 T cells in the spleen. In addition, it has been demonstrated that IP-10 is a critical factor in the pathogenesis of experimental autoimmune encephalomyelitis (35–37), mouse hepatitis virus-induced encephalomyelitis (38), and adjuvant arthritis (39). Recently, it was also reported that CXCR3 is required for the infiltration of the islets of Langerhans and the subsequent development of diabetes in RIP-LCMV mice (40). It was shown that the onset of diabetes was delayed in CXCR3-deficient mice and that β cells may be responsible for the CXCR3-mediated infiltration of autoaggressive lymphocytes. Our studies extend and clarify this observation by showing that neutralization of just one particular CXCR3 chemokine, namely IP-10, is responsible for abrogation of type 1 diabetes in RIP-LCMV mice. Furthermore, we revealed that the mechanism by which this occurs is through a reduction in the expansion of Ag-specific CD8 T cells in the spleen and their subsequent migration into the pancreas. Thus, neutralization of one component in the innate immune response can impair the programming of the Ag-specific adaptive immune response and therefore can prevent a virus infection from causing an autoimmune disease.

Recent interest has refocused on the hypothesis that distressed or injured cells release alarm signals that in turn activate the resting immune system (41). Our results support this hypothesis and indicate that IP-10 is an early alarm signal for LCMV infection in the pancreas. Others reported that CVB infection of the pancreas

initiated and potentiated diabetes in the BDC2.5 transgenic nonobese diabetic mouse by bystander damage as a result of local inflammation (42, 43). However, the precise factors contributing to the acceleration of diabetes were not determined. As an extension of these findings, we found a massive elevation of IP-10 expression in the pancreas of C57BL/6 mice 4 days after infection with CVB. Furthermore, secondary infection of RIP-LCMV-NP mice (10) with CVB 1 mo after an initial infection with LCMV significantly accelerated and enhanced the course of diabetes. However, CVB alone was unable to initiate type 1 diabetes in the RIP-LCMV model and CVB does not contain an epitope that mimics an LCMV T cell epitope. These results suggest, like the report by Horwitz et al. (42), that once autoaggressive (anti-LCMV) T cells are formed after the primary LCMV infection, a later infection by an unrelated virus with tropism for the pancreas results in the release of additional alarm signals, such as IP-10. As shown here, IP-10 can then contribute to the expansion of autoaggressive T cells and enhance their migration into the islets. Blocking IP-10 is associated with a reduction in the number of Ag-specific T cells required to cause diabetes. Hence, our findings with IP-10 noted in the RIP-LCMV mouse may be relevant for understanding the pathogenesis of human type 1 diabetes and perhaps other autoimmune diseases.

References

1. Zlotnik, A., and O. Yoshie. 2000. Chemokines: a new classification system and their role in immunity. *Immunity 12:121*.
2. O'Garra, A., L. M. McEvoy, and A. Zlotnik. 1998. T-cell subsets: chemokine receptors guide the way. *Curr. Biol. 8:R646*.
3. Loetscher, P., M. Uguccioni, L. Bordoli, M. Baggiolini, B. Moser, C. Chizzolini, and J. M. Dayer. 1998. CCR5 is characteristic of Th1 lymphocytes. *Nature 391:344*.
4. Bonecchi, R., G. Bianchi, P. P. Bordignon, D. D'Ambrosio, R. Lang, A. Borsatti, S. Sozzani, P. Allavena, P. A. Gray, A. Mantovani, and F. Sinigaglia. 1998. Differential expression of chemokine receptors and chemotactic responsiveness of type 1 T helper cells (Th1s) and Th2s. *J. Exp. Med. 187:129*.
5. Sallusto, F., D. Lenig, C. R. Mackay, and A. Lanzavecchia. 1998. Flexible programs of chemokine receptor expression on human polarized T helper 1 and 2 lymphocytes. *J. Exp. Med. 187:875*.
6. D'Ambrosio, D., A. Iellem, R. Bonecchi, D. Mazzeo, S. Sozzani, A. Mantovani, and F. Sinigaglia. 1998. Selective up-regulation of chemokine receptors CCR4 and CCR8 upon activation of polarized human type 2 Th cells. *J. Immunol. 161:5111*.
7. Imai, T., M. Nagira, S. Takagi, M. Kakizaki, M. Nishimura, J. Wang, P. W. Gray, K. Matsushima, and O. Yoshie. 1999. Selective recruitment of CCR4-bearing Th2 cells toward antigen-presenting cells by the CC chemokines thymus and activation-regulated chemokine and macrophage-derived chemokine. *Int. Immunol. 11:81*.
8. Ohashi, P., S. Oehen, K. Buerki, H. Pircher, C. Ohashi, B. Odermatt, B. Malissen, R. Zinkernagel, and H. Hengartner. 1991. Ablation of tolerance and induction of diabetes by virus infection in viral antigen transgenic mice. *Cell 65:305*.
9. Oldstone, M. B. A., M. Nerenberg, P. Southern, J. Price, and H. Lewicki. 1991. Virus infection triggers insulin-dependent diabetes mellitus in a transgenic model: role of anti-self (virus) immune response. *Cell 65:319*.
10. von Herrath, M. G., J. Dockter, and M. B. A. Oldstone. 1994. How virus induces a rapid or slow onset insulin-dependent diabetes mellitus in a transgenic model. *Immunity 1:231*.
11. Seewaldt, S., H. Thomas, M. Ejrnaes, U. Christen, T. Wolfe, E. Rodrigo, B. Coon, B. Michelsen, T. Kay, and M. G. von Herrath. 2000. Virus-induced autoimune diabetes: most β-cells die through inflammatory cytokines and not perforin from autoreactive (anti-viral) CTL. *Diabetes 49:1801*.
12. Christen, U., T. Wolfe, U. Mohrle, A. C. Hughes, E. Rodrigo, E. A. Green, R. A. Flavell, and M. G. von Herrath. 2001. A dual role for TNF-α in type 1 diabetes: islet-specific expression abrogates the ongoing autoimmune process when induced late but not early during pathogenesis. *J. Immunol. 166:7023*.
13. von Herrath, M. G., and A. Holz. 1997. Pathological changes in the islet milieu precede infiltration of islets and destruction of β-cells by autoreactive lymphocytes in a transgenic model of virus-induced IDDM. *J. Autoimmun. 10:231*.
14. Lane, T. E., V. C. Asensio, N. Yu, A. D. Paoletti, I. L. Campbell, and M. J. Buchmeier. 1998. Dynamic regulation of α- and β-chemokine expression in the central nervous system during mouse hepatitis virus-induced demyelinating disease. *J. Immunol. 160:970*.
15. Asensio, V. C., and I. L. Campbell. 1997. Chemokine gene expression in the brains of mice with lymphocytic choriomeningitis. *J. Virol. 71:7832*.
16. Hoffman, L. M., B. T. Fife, W. S. Begolka, S. D. Miller, and W. J. Karpus. 1999. Central nervous system chemokine expression during Theiler's virus-induced demyelinating disease. *J. Neurovirol. 5:635*.
17. McGavern, D. B., U. Christen, and M. B. Oldstone. 2002. Molecular anatomy of antigen-specific $CD8^+$ T cell engagement and synapse formation in vivo. *Nat. Immunol. 3:918*.
18. Okabe, M., M. Ikawa, K. Kominami, T. Nakanishi, and Y. Nishimune. 1997. "Green mice" as a source of ubiquitous green cells. *FEBS Lett. 407:313*.
19. Pircher, H., K. Burki, R. Lang, H. Hengartner, and R. M. Zinkernagel. 1989. Tolerance induction in double specific T-cell receptor transgenic mice varies with antigen. *Nature 342:559*.
20. Jun, H. S., Y. Kang, H. S. Yoon, K. H. Kim, A. L. Notkins, and J. W. Yoon. 1998. Determination of encephalomyocarditis viral diabetogenicity by a putative binding site of the viral capsid protein. *Diabetes 47:576*.
21. Khan, I. A., J. A. MacLean, F. S. Lee, L. Casciotti, E. DeHaan, J. D. Schwartzman, and A. D. Luster. 2000. IP-10 is critical for effector T cell trafficking and host survival in *Toxoplasma gondii* infection. *Immunity 12:483*.
22. von Herrath, M. G., S. Guerder, H. Lewicki, R. Flavell, and M. B. A. Oldstone. 1995. Coexpression of B7.1 and viral (self) transgenes in pancreatic β-cells can break peripheral ignorance and lead to spontaneous autoimmune diabetes. *Immunity 3:727*.
23. Laufer, T. M., M. G. von Herrath, M. J. Grusby, M. B. Oldstone, and L. H. Glimcher. 1993. Autoimmune diabetes can be induced in transgenic major histocompatibility complex class II-deficient mice. *J. Exp. Med. 178:589*.
24. Klavinskis, L. S., J. L. Whitton, E. Joly, and M. B. Oldstone. 1990. Vaccination and protection from a lethal viral infection: identification, incorporation, and use of a cytotoxic T lymphocyte glycoprotein epitope. *Virology 178:393*.
25. Murali-Krishna, K., J. D. Altman, M. Suresh, D. J. Sourdive, A. J. Zajac, J. D. Miller, J. Slansky, and R. Ahmed. 1998. Counting antigen-specific CD8 T cells: a reevaluation of bystander activation during viral infection. *Immunity 8:177*.
26. Homann, D., L. Teyton, and M. B. Oldstone. 2001. Differential regulation of antiviral T-cell immunity results in stable $CD8^+$ but declining $CD4^+$ T-cell memory. *Nat. Med. 7:913*.
27. von Herrath, M. G., B. Coon, and T. Wolfe. 2001. Tolerance induction with agonist peptides recognized by autoaggressive lymphocytes is transient: therapeutic potential for type 1 diabetes is limited and depends on time-point of administration, choice of epitope and adjuvant. *J. Autoimmun. 16:193*.
28. Aichele, P., D. Kyburz, P. S. Ohashi, B. Odermatt, R. M. Zinkernagel, H. Hengartner, and H. Pircher. 1994. Peptide-induced T-cell tolerance to prevent autoimmune diabetes in a transgenic mouse model. *Proc. Natl. Acad. Sci. 91:444*.
29. Haanen, J. B., M. G. van Oijen, F. Tirion, L. C. Oomen, A. M. Kruisbeek, F. A. Vyth-Dreese, and T. N. Schumacher. 2000. In situ detection of virus- and tumor-specific T-cell immunity. *Nat. Med. 6:1056*.
30. Skinner, P. J., M. A. Daniels, C. S. Schmidt, S. C. Jameson, and A. T. Haase. 2000. Cutting edge: In situ tetramer staining of antigen-specific T cells in tissues. *J. Immunol. 165:613*.
31. Liu, M. T., D. Armstrong, T. A. Hamilton, and T. E. Lane. 2001. Expression of Mig (monokine induced by interferon-γ) is important in T lymphocyte recruitment and host defense following viral infection of the central nervous system. *J. Immunol. 166:1790*.
32. Loetscher, M., B. Gerber, P. Loetscher, S. A. Jones, L. Piali, I. Clark-Lewis, M. Baggiolini, and B. Moser. 1996. Chemokine receptor specific for IP10 and Mig: structure, function, and expression in activated lymphocytes. *J. Exp. Med. 184:963*.
33. Qin, S., J. B. Rottman, P. Myers, N. Kassam, M. Weinblatt, M. Loetscher, A. E. Koch, B. Moser, and C. R. Mackay. 1998. The chemokine receptors CXCR3 and CCR5 mark subsets of T cells associated with certain inflammatory reactions. *J. Clin. Invest. 101:746*.
34. Dufour, J. H., M. Dziejman, M. T. Liu, J. H. Leung, T. E. Lane, and A. D. Luster. 2002. IFN-γ-inducible protein 10 (IP-10; CXCL10)-deficient mice reveal a role for IP-10 in effector T cell generation and trafficking. *J. Immunol. 168:3195*.
35. Fife, B. T., K. J. Kennedy, M. C. Paniagua, N. W. Lukacs, S. L. Kunkel, A. D. Luster, and W. J. Karpus. 2001. CXCL10 (IFN-γ-inducible protein-10) control of encephalitogenic $CD4^+$ T cell accumulation in the central nervous system during experimental autoimmune encephalomyelitis. *J. Immunol. 166:7617*.
36. Wildbaum, G., N. Netzer, and N. Karin. 2002. Plasmid DNA encoding IFN-γ-inducible protein 10 redirects antigen-specific T cell polarization and suppresses experimental autoimmune encephalomyelitis. *J. Immunol. 168:5885*.
37. Narumi, S., T. Kaburaki, H. Yoneyama, H. Iwamura, Y. Kobayashi, and K. Matsushima. 2002. Neutralization of IFN-inducible protein 10/CXCL10 exacerbates experimental autoimmune encephalomyelitis. *Eur. J. Immunol. 32:1784*.
38. Liu, M. T., H. S. Keirstead, and T. E. Lane. 2001. Neutralization of the chemokine CXCL10 reduces inflammatory cell invasion and demyelination and improves neurological function in a viral model of multiple sclerosis. *J. Immunol. 167:4091*.
39. Salomon, I., N. Netzer, G. Wildbaum, S. Schif-Zuck, G. Maor, and N. Karin. 2002. Targeting the function of IFN-γ-inducible protein 10 suppresses ongoing adjuvant arthritis. *J. Immunol. 169:2685*.
40. Frigerio, S., T. Junt, B. Lu, C. Gerard, U. Zumsteg, G. A. Hollander, and L. Piali. 2002. β Cells are responsible for CXCR3-mediated T-cell infiltration in insulitis. *Nat. Med. 8:1414*.
41. Matzinger, P. 2002. The danger model: a renewed sense of self. *Science 296:301*.
42. Horwitz, M. S., L. M. Bradley, J. Harbertson, T. Krahl, J. Lee, and N. Sarvetnick. 1998. Diabetes induced by Coxsackie virus: initiation by bystander damage and not molecular mimicry. *Nat. Med. 4:781*.
43. Serreze, D. V., E. W. Ottendorfer, T. M. Ellis, C. J. Gauntt, and M. A. Atkinson. 2000. Acceleration of type 1 diabetes by a Coxsackievirus infection requires a preexisting critical mass of autoreactive T-cells in pancreatic islets. *Diabetes 49:708*.